

# Wear Properties of Aluminum Alloy 211z.1 Drilling Tool

Yong Liu<sup>1</sup>, Lin He<sup>2\*</sup>, Sen Yuan<sup>3</sup>

<sup>1</sup>College of Mechanical Engineering, Guizhou University, Guiyang, 550025, China

<sup>2</sup>School of Mining and Civil Engineering, Liupanshui Normal College, Liupanshui 553004, China

<sup>3</sup>College of Mechanical Engineering, Guizhou Institute of Technology, Guiyang 550003, China

Received July 18 2020

Accepted Feb 20 2021

## Abstract

In the application process of China's independently produced new aluminum alloy 211z.1 into high-end military and civilian industries, a great many holes are needed for fastening connection. However, the severe wear of the cutting edge of twist drill is an important factor that restricts the quality of hole processing and tool life. In this paper, the wear condition of the standard high-speed steel twist drill in drilling the new aluminum alloy 211z.1 is studied based on the drilling test, and the influence law of the drilling amount on the tool wear is revealed by designing a reasonable drilling test plan. The research results show that the cutting speed has a significant effect on the flank wear, and the drilling feed and the drilling height have relatively little influence on the flank wear of the tool.

© 2021 Jordan Journal of Mechanical and Industrial Engineering. All rights reserved

**Keywords:** Aluminum Alloy 211z.1; High-speed Steel; Standard Twist Drill; Drilling Test; Flank Wear;

## 1. Introduction

Drilling is a commonly used processing method in production, it is one of the most important processes in metal cutting (accounting for about one-third of all metal cutting processes), and billions of drills are consumed every year in the world<sup>[1]</sup>. As early as in the 1960s, a large number of experimental studies on the processing of aluminum alloy, especially in the precision of hole making and surface integrity, were carried out from the aspects of tools, process methods, lubrication conditions, etc. As a widely used free-cutting material, especially with the emergence of various new aluminum alloy materials, the analysis of the drilling tool wear situation is still of great significance in the large-volume, continuous drilling process<sup>[2]</sup>.

Aluminum alloy 211z.1 is one of the five registered grades of the 211z.x series independently developed by China, and it belongs to the new high-strength aluminum alloy materials of Al-Cu-Mn series. The main chemical composition is shown in Table 1<sup>[3]</sup>. At present, a lot of research has been done on the phase transformation<sup>[4-5]</sup>, high temperature mechanical properties<sup>[6-7]</sup>, fatigue properties<sup>[8]</sup> and microstructure properties<sup>[9-10]</sup> of the new aluminum alloy 211z.1. However, there are few studies on the cutting performance of the aluminum alloy, except for the processing methods of aluminum alloy such as turning<sup>[11]</sup> and milling<sup>[12]</sup>, it is necessary to further expand the research scope and increase the research on the cutting performance

of cast aluminum alloy, thus providing a theoretical basis for increasing the application of the aluminum alloy material in various high-end military and civilian industries and fields.

Based on theoretical analysis and drilling experiment results, the wear pattern of the tool during the processing of aluminum alloy 211z.1 is analyzed in this paper by using the standard high-speed steel twist drill, and a quadratic polynomial regression prediction model for the  $VB_{Bmax}$  wear value of the flank was constructed by orthogonal test and linear regression analysis by taking the flank wear amount as the research object.

## 2. Drilling Test Plan

Aluminum alloy 211z.1 is produced by Guizhou Hualco Aluminum Co., Ltd., and its main mechanical properties are shown in Table 2<sup>[3]</sup>. The upper surface of the processed workpiece is flat, the size is 145 mm × 160 mm × 45 mm, and the V850A numerical control (vertical) machining center is adopted as the drilling experiment tool. The high-speed steel twist drill meets the technical standard of GB t 17984-2000. The tool diameter  $d = 8, 10$  and 12mm for analyzing the drilling wear phenomenon of aluminum alloy 211z.1, and the tool diameter  $d = 10$ mm for calculating the tool wear prediction model. Dry cutting and blindhole drilling are adopted in the experiment. Jerry DJCL Y92B detector and DMSZ7 video all-in-one machine are adopted as the tool wear detection device.

\* Corresponding author e-mail: helin6568@163.com.

### 3. Breakage Form Analysis of Aluminum Alloy 211z.1 Drilling Tool

The twist drill is a complex-form double-edged boring tool that performs a semi-closed cutting pattern with cutting temperatures higher than the other cutting forms (such as turning, milling, etc.) under the same cutting conditions. Under the action of uneven high-field thermal coupling, the cutting load on the cutting edge is very uneven, and different areas of the cutting edge have different wear properties in different processing stages. In the continuous processing, with the parameter change of different processing objects, tool materials, pore sizes and processing, the form and characteristics of wear vary greatly, and the wear law is complex, often appear one wear pattern with many other forms of wear.

#### 3.1. Chisel edge wear

In the drilling process of aluminum alloy 211z.1 and the pre-use of tool under the same working condition, the twist

drill's chisel edge that plays the main function of positioning, centering and reducing the chattering effect during processing first contacts the material being processed. While rotating around the central shaft, the chisel edge crushes and scrapes the materials being cut, causing severe deformation, and the force of contact and thermal stress between the cutting edges of the tool are concentrated, and then a triangular-like smooth surface is quickly grinded out on both sides accompanied by bonding of aluminum alloy materials, forming a built-up edge, as shown in Figure 1. The hardness of the built-up edge is generally 2-3 times the hardness of the workpiece, and the built-up edge is stacked on the cutting edge to replace the cutting edge in cutting and protecting the cutting edge, and to increase the actual working front angle and reduce the cutting deformation<sup>[13-15]</sup>. The blunt circular cutting edge formed by stacking causes extrusion and overcutting, which reduces the processing accuracy, and the built-up edge is adhered to the processed surface after detaching, resulting in the surface roughness and unevenness.

**Table 1.** Chemical composition of aluminum alloy 211z.1<sup>[3]</sup>

Elemnt	Cu	Mn	Ti	Zr	B <sup>a</sup>	C <sup>a</sup>	Cd
%	4.0-7.5	0.20-0.6	0.05-0.40	0.05-0.50	0.005-0.07	0.003-0.005	0.05-0.50
Elemnt	RE	Be	Fe	Si	Other <sup>b</sup>		Al <sup>c</sup>
					single	total	
%	0.02-0.30	0.001-0.08	≤0.30	≤0.10	≤0.05	≤0.15	Rest

**Table 2** Mechanical properties of aluminum alloy 211z.1<sup>[3]</sup>

Sample state	Tensile properties at room temperature		Tensile properties at high temperature (350°C)		Hardness (HBW)	Shock absorption energy (KU <sub>2</sub> )/J
	Tensile strength R <sub>m</sub> /MPa	Elongation after break A/%	Tensile strength R <sub>m</sub> /MPa	Elongation after break A/%		
No less than						
T5	450	8	130	6	125	6.5

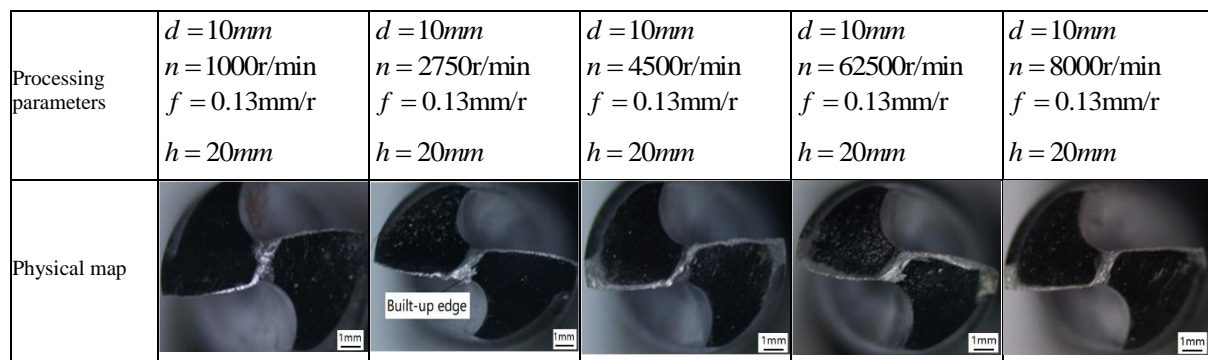


**Figure 1.** Physical map of chisel edge wear and built-up edge

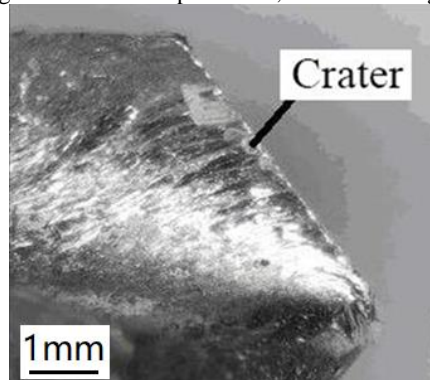
### 3.2. Flank wear

In the drilling process of aluminum alloy 211z.1, the main flank of the twist drill is in continuous contact with the material being cut. Under the axial feed force and the rotational driving force, severe deformation and friction is caused between the tool and the material being cut, increasing the temperature and internal pressure in the contact zone and causing wear on the flank of the twist drill. The flank wear of the twist drill appears uneven wear distribution affected by the complex structure of the twist drill's flank, and by the rotating and feeding composite spiral motion form. The flank wear of the main cutting edge is usually fanshaped with wear or a strip with an approximately uniform shape and a smaller width, as shown in Figure 2. The outermost edge of the main cutting edge has the largest rake angle, the highest cutting line speed, the heaviest cutting load and the highest cutting temperature, which is easy to form corner wear, as shown in Figure 3. The outer edge of the twist drill has the most serious wear, and the width of the wear band is the largest. When the rotational speed is high, the temperature and friction velocity of the outer edge increase, the thermal wear is intensified, and obvious "ablation" occurs, these observations are similar to that found by other researchers [16-17].

### 3.3. Rake wear

In the drilling process of aluminum alloy 211z.1, the contact surface between the tool and the chips has an inner friction zone and an outer friction zone, namely, a bonding zone and a sliding zone. The outer friction zone of sliding is away from the cutting edge, and the cutting temperature of

which is lower than the temperature at the cutting edge, the heat dissipation is relatively fast, and sliding friction is formed between the chips and the tool, and thus the tool rake is less damaged; the inner friction zone of sliding is where the relative movement of the tool and the material occurs, high temperature and high pressure (2-3 GPa) are formed under the action of friction and extrusion. Under the affinity (cold welding) of the material is formed, which is prone to bond and spread wear, causing craters on the rake area that is close to the main cutting edge. In addition, due to the semi-closed cutting form, the heat cannot be dissipated and discharged in time, causing the twist drill temperature to rise and chips to accumulate in the chip pocket and to adhere to the rake, aggravating the bonding and wear of the rake while making the craters more prominent, as shown in Figure 4.



$d = 8mm, n = 1000r/min, f = 0.13mm/r, h = 15mm$   
 Drilling conditions:  $d = 8mm, n = 1000r/min, f = 0.13mm/r, h = 15mm$

Figure 4. Physical map of the rake wear band of twist drill

Processing parameters	$d = 8mm$ $n = 4500r/min$ $f = 0.1mm/r$ $h = 10mm$	$d = 8mm$ $n = 4500r/min$ $f = 0.2mm/r$ $h = 10mm$	$d = 10mm$ $n = 4500r/min$ $f = 0.2mm/r$ $h = 15mm$	$d = 12mm$ $n = 8000r/min$ $f = 0.2mm/r$ $h = 10mm$	$d = 12mm$ $n = 8000r/min$ $f = 0.2mm/r$ $h = 20mm$
Physical map					

Figure 2. Physical map of the flank wear band after continuous drilling of 30 blind holes

Processing parameters	$d = 12mm$ $n = 2750r/min$ $f = 0.25mm/r$ $h = 20mm$	$d = 12mm$ $n = 4500r/min$ $f = 0.25mm/r$ $h = 20mm$	$d = 12mm$ $n = 6250r/min$ $f = 0.25mm/r$ $h = 20mm$	$d = 12mm$ $n = 4500r/min$ $f = 0.05mm/r$ $h = 20mm$	$d = 12mm$ $n = 4500r/min$ $f = 0.15mm/r$ $h = 20mm$
Physical map					

Figure 3. Physical map of the outer edge corner after continuous drilling of 30 blind holes

#### 4. Prediction Model of Flank Wear

As shown in Figure 5, the cross cutting edge angle between the cross cutting edge and the main cutting edge is taken as the measurement reference, and the wear value of flank  $VB_{Bmax}$  is taken as the research object, and the orthogonal drilling experiment is conducted, the  $VB_{Bmax}$  is measured according to different drilling processing parameters, and the flank wear prediction model is analyzed. Each group of experiments is repeated three times, and the average value is taken as the experimental result, as shown in Table 3.

**Table 3.** Parameters and flank wear values of the orthogonal drilling experiment

Plan	$v$ (m/min)	$f$ (mm/r)	$h$ (mm)	$VB_{Bmax}$ (mm)
1	250	0.13	10	0.4046
2	140	0.13	15	0.3217
3	250	0.2	15	0.8802
4	30	0.13	10	0.0932
5	140	0.13	15	0.3217
6	140	0.2	20	0.5522
7	140	0.05	10	0.2054
8	140	0.2	10	0.3387
9	250	0.05	15	0.3586
10	30	0.05	15	0.0439
11	140	0.05	20	0.3121
12	140	0.13	15	0.3217
13	140	0.13	15	0.3217
14	140	0.13	15	0.3217
15	30	0.2	15	0.1355
16	30	0.13	20	0.1744
17	250	0.13	20	0.9196

Note:  $v$ -cutting speed,  $f$ -feed,  $h$ -drilling height

The regression analysis on the experimental data of Table 3 is performed by using the Design Expert software, and the quadratic polynomial regression prediction model of the flank  $VB_{Bmax}$  wear value is obtained as follows:

$$\left\{ \begin{array}{l} VB_{Bmax} = 0.59101 - 3.13476 \times 10^{-3} \times v - 1.02093 \times f - 0.057065 \times h \\ + 0.013194 \times v \times f + 1.97182 \times 10^{-4} \times v \times h + 0.0712 \times f \times h \\ + 3.30785 \times 10^{-6} \times v^2 - 1.03556 \times f^2 + 1.449 \times 10^{-3} \times h^2 \\ 30 \leq v \leq 250 \\ 0.05 \leq f \leq 0.2 \\ 10 \leq h \leq 20 \end{array} \right.$$

As shown in Table 4, a significance analysis of the regression model established is conducted, and the correction coefficient of the flank wear model is 0.982. The model can only reflect 98.2% of the relationship between the factor and the response value, and the influence of each factor on the flank wear is ranked as: cutting speed > feed >

drilling height. The variable coefficient of the flank wear model response is 13.64%, and the experiment has a certain degree of reliability, thus the prediction model can be used for the analysis and prediction of flank wear of the aluminum alloy 211z.1 drilling tool.

The response surface diagram and contour map of the interaction of drilling parameters on flank wear are obtained by quadratic multiple regression fitting, as shown in Figure 6. The rise of the three response surfaces is obvious, and the curvature radius of the contour line is large, indicating that  $f$  and  $v$ ,  $h$  and  $v$ ,  $h$  and  $f$  have significant interaction effects on flank wear. As  $v$  increases, flank wear increases obviously; with the increase of  $f$  and  $h$ , the increase of flank wear is not obvious.

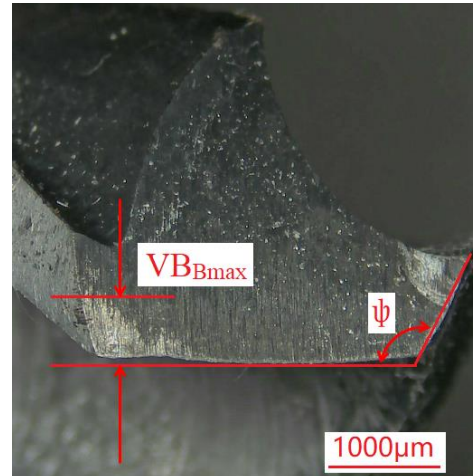


**Figure 5.** Measurement of wear band on flank of main cutting edge

#### 5. Conclusion

1. The normal wear pattern of aluminum alloy 211z.1 drilling tool includes chisel edge wear, rake wear and flank wear, among which chisel edge wear appears first, accompanied by built-up edge; rake wear is usually accompanied by craters; and flank wear has a wide range, and the most worn parts are in the outer corner area. The aluminum alloy 211z.1 often occurs "sticking on tools" during the drilling process.
2. Based on the flank wear amount, a prediction model of aluminum alloy 211z.1 drilling flank wear is constructed, which ranks the influence of each factor on flank wear as follows: cutting speed > feed > drilling height.

**Table 4.** Checklist of the regression model

	Source of variance	Sum of squares	Degree of freedom	Mean square	F value	P value	Significance
$VB_{Bmax}$	Model	0.89	9	0.099	42.35	< 0.0001	Significant
	$v$	0.56	1	0.56	237.80	< 0.0001	
	$f$	0.12	1	0.12	51.40	0.0002	
	$h$	0.10	1	0.10	44.83	0.0003	
	Residual	0.016	7	2.342E-003			

$R^2 = 0.9820$ ,  $R^2_{adj} = 0.9588$ ,  $CV\% = 13.64$

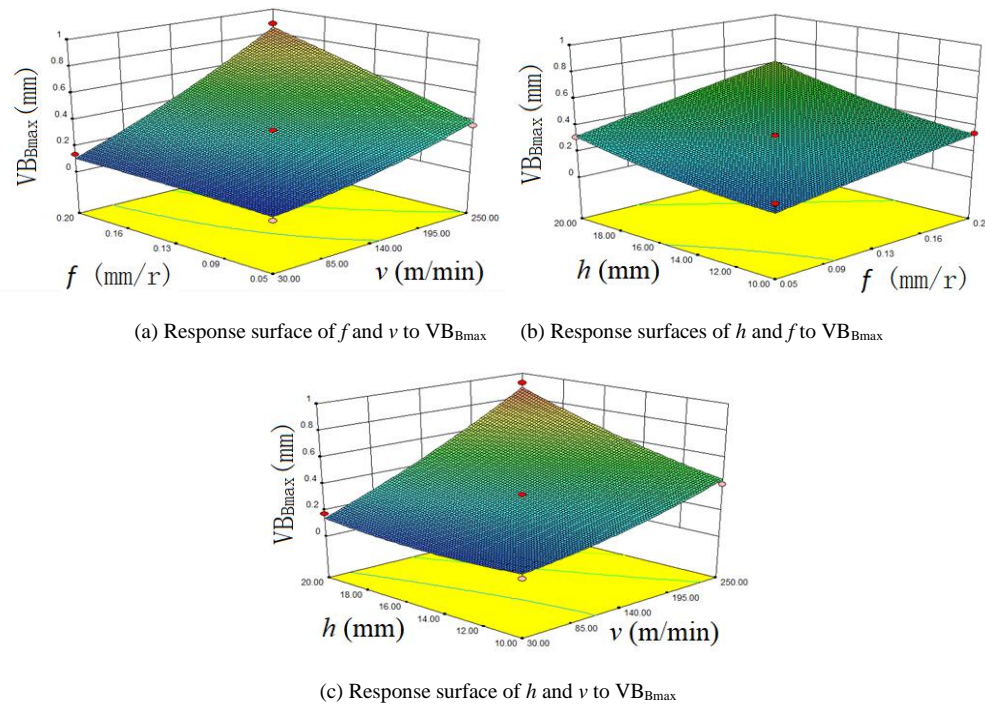


Figure 6. Multi-factor interactive response surface map

### Acknowledgement

Supported by the projects of National Natural Science Foundation of China (51765009).

### References

- [1] Liu J.A. Discussion on the development trend of aluminum alloy materials and processing industry and technology (I). *Aluminum Machining*, 2012, 1(204): 13-18.
- [2] Davim J.P., Sreejith P.S., Gomes R., and Peixoto C. Experimental studies on drilling of aluminium (AA1050) under dry, minimum quantity of lubricant, and flood-lubricated conditions. *Proceedings of the Institution of Mechanical Engineers Part B Journal of Engineering Manufacture*, 2006, 220(10): 1605-1611.
- [3] Li R.H., Zeng P., and Li J.D. Interpretation of the national standard of aluminum alloy ingot for heat-resistant high-strength and toughness castings. *Casting*, 2013, 8(62): 811-813.
- [4] Wu Y.F., Liu K.J., Zhang Z.K., Li Q., and Fu Y.Y. Thermal energy analysis: phase transformation of an Al-Cu alloy. *Shanghai Metals*, 2013, (3): 27-30.
- [5] Zhang Z.K., Che Y., Men S.Q., and Chen X.M. Aging precipitates in Al-Cu-Mn high strength aluminum alloy. *Special Casting and Nonferrous Alloy*, 2014, 34(10): 1114-1116.
- [6] Zhang Z.K., Che Y., Men S.Q., and Li X. High temperature mechanical properties of Al-Cu-Mn cast aluminum alloy. *Hot Working Technology*, 2012, 41(19): 8-10.
- [7] Xu X., Yang M., Liang Y.L., Zhang S.W., and Gong Q.J. Research on hot compressive deformation and processing map of 211Z.X heat-resisting high strength aluminium alloy. *Materials guide B: Research*, 2016, 30(9): 143-148.
- [8] Zhang X.M., Mao J., Che Y., and Zhang Z.K. Investigations on the fatigue property of the high-strength and toughness 211Z casting aluminum alloy. *Applied Mechanics and Materials*, 2013, 197-201.
- [9] Wu X.Y., Mao J., Che Y., and Zhang Z.K. Effect of solution time on properties of 211Z hot extrusion deformed aluminum alloy. *Hot Working Technology*, 2014, 43(10): 191-193.
- [10] Cheng X.H., Mao J., Che Y., and Zhang Z.K. Effect of extrusion-heat on intergranular corrosion of 211Z aluminum alloy. *Transactions of Materials and Heat Treatment*, 2015, 36(1): 63-66.
- [11] Zhang R.R. Effect of turning process parameters on surface quality of aluminum alloy 211Z. *Guiyang: Guizhou University*, 2016, 143-148.
- [12] Tang Q.Q., Zhao X.F., Wang D.D., and Huang Q. Experimental study on the influence of milling parameters on surface roughness of aluminum alloy. *Machinery Design and Manufacture*, 2016, 9(9): 134-136.
- [13] Wang H. Deep drainage detection system for inland vessels based on machine vision. *Jordan Journal of Mechanical and Industrial Engineering*, 2020, 14(1): 119-128.
- [14] Prasad, G., and Das, A. Design approach of shell and tube vaporizer for LNG regasification. *Jordan Journal of Mechanical and Industrial Engineering*, 2018, 12(2): 109-116.
- [15] Xu X.W., and Wang Q.M. On the influence of chip accumulation on machining accuracy. *Science & Technology Information*, 2010, (17): 627-628.
- [16] Zhang Y.Z. *Metal cutting theory*. Aviation Industry Press, 1988.
- [17] Liu L.Y., Wang J.F., Tu Z.B., Qing Z.H., and Ye Z. Study on the roughness of the machined surface and wear mechanism of the cutter in dry cutting aluminum alloy with YG8 cemented carbide. *Technology and Test*, 2018, (6): 120-123.